Dyes and Pigments 98 (2013) 42–50

Contents lists available at SciVerse ScienceDirect

Dyes and Pigments

journal homepage: www.elsevier.com/locate/dyepig

New fluorescent and colorimetric chemosensors based on the rhodamine detection of Hg^{2+} and Al^{3+} and application of imaging in living cells

Fanyong Yan [a,*], Meng Wang [a], Donglei Cao [a], Ning Yang [a], Yang Fu [a], Li Chen [a,*], Ligong Chen [b]

[a] State Key Laboratory of Hollow Fiber Membrane Materials and Processes, Key Lab of Fiber Modification & Functional Fiber of Tianjin, Tianjin Polytechnic University, Tianjin 300387, China
[b] School of Chemical Engineering, Tianjin University, Tianjin 300072, China

ARTICLE INFO

Article history:
Received 7 December 2012
Received in revised form
31 January 2013
Accepted 1 February 2013
Available online 16 February 2013

Keywords:
Fluorescent sensor
Mercury
Aluminum
Rhodamine
Phthalimido acids
Cellular imaging

ABSTRACT

Employing the "Off–On" switching of the spirocyclic moiety in Rhodamine B derivatives, three sensors were designed and characterized as new fluorescent probes for detecting Hg^{2+} and Al^{3+} in the environment, respectively. The first probe exhibited chromogenic and fluorogenic selectivity to detection of Hg^{2+} in methanol-H_2O (4:6, v/v, HEPES, pH 7.0). The first and second probes displayed fluorescence intensity enhancement following Hg^{2+} coordination with limits of detection for Hg^{2+} at the ppb level. The limit of detection based on 3 blank/k was calculated to be 2.5×10^{-8} M and 4.2×10^{-8} M, respectively. The third probe contained a benzyl group which resulted in better selectivity for Al^{3+}. Job's plot clearly suggested the formation of 1:1 complexation behavior between the three probes and Hg^{2+} or Al^{3+}. The three probes can be used as a fluorescent probe for monitoring Hg^{2+} or Al^{3+} in living cells with satisfying results, which demonstrates the value of the probes in practical applications in environmental and biological systems.

1. Introduction

The design of chemosensors for the detection of heavy and transition metal ions are particularly attractive, because these ions play important roles in living systems and have an extremely toxic impact on the environment [1–4]. Among transition-metal ions, mercury is considered as one of the most dangerous cations for the environment. Mercury can accumulate in the human body, its high affinity for thiol groups in proteins and enzymes lead to the dysfunction of cells and consequently causing health problems, such as prenatal brain damage, serious cognitive and minamata disease [5–7]. Al^{3+} widely exists within the environment due to acidic rain and human activities. The increase of Al^{3+} concentration in the environment is not only detrimental to growing plants but also damages many biological functions. Excessive exposure of the human body to Al^{3+} leads to a wide range of diseases, such as Alzheimer's disease, Parkinson's disease, etc. [8–10].

Many detection methods for the quantitative analysis of Hg^{2+} in water samples include atomic absorption spectroscopy, cold vapor atomic fluorescence spectrometry, and gas chromatography, which usually require complicated, multistep sample preparation and sophisticated instrumentation [11–14]. Fluorescence analysis offers significant advantages over other methods for metal ion detection and measurement due to its simplicity, high sensitivity, low cost and instantaneous response [15].

In recent years, progress in the area of chemosensors has contributed significantly to the development of a variety of Al^{3+} sensors based on triazole, Schiff's base and coumarin Refs. [16–18]. Unfortunately, some of the Al^{3+} sensors have disadvantages such as poor water-solubility or UV light excitation [8,19,20]. So few Al^{3+} sensors have been reported up to now. Mercury-selective fluorescent sensors have been reported in the past where in most cases the presence of mercury can cause fluorescence quenching of the fluorophores via the spin orbit coupling effect or complicated synthesis methods [21–23]. Therefore, overcoming these disadvantages in the development of excellent sensors for the sensitive and selective determination of Hg^{2+} and Al^{3+} is a challenging task.

In the form of proteins, amino acids comprise the second largest component other than water of human muscles, cells and other tissues.

* Corresponding authors. Tel.: +86 22 83955766; fax: +86 22 83955016.
E-mail addresses: yfytju@yahoo.com (F. Yan), chenlis11@yahoo.com.cn (L. Chen).

0143-7208/$ – see front matter © 2013 Elsevier Ltd. All rights reserved.
http://dx.doi.org/10.1016/j.dyepig.2013.02.002

As amino acids have both a primary amine group and a primary carboxyl group, these chemicals can undergo most of the reactions associated with these functional groups [24]. These include amide bond formation and decarboxylation for the carboxylic acid group. The combination of these functional groups allowed amino acids to be effective ligands for metal-amino acid chelates. Because of their biological significance, amino acids are also used to chelate metal cations in order to improve the ability of a probe to detect metals [25–30].

Due to the structure and behavior of rhodamine and related derivatives [31–33], rhodamine can make an ideal model to use in constructing chelation-enhanced fluorescence "Off–On" switch sensors for metal ions. Without cations, these rhodamine-based chemosensors exist in a spirocyclic form which is colorless and non-fluorescent. The addition of a specific metal ion leads to spirocycle opening via a reversible coordination or an irreversible chemical reaction [34–39], resulting in intense fluorescence emission and development of pink color. However, the rhodamine-based derivatives may lead to self-quenching and fluorescence detection errors because of excitation back-scattering effects [40].

Thus, it is important to have sensors with improved properties. In our previous work, we have reported an excellent rhodamine-based fluorescent sensor for Hg^{2+} in aqueous solution [41]. Compared with the fluorescent probe Rh–C which had been reported by our group, RW1 exhibited much better fluorescence selectivity toward Hg^{2+} and bio-compatibility, and much lower detection limit (2.5×10^{-8} M). Herein, we synthesized the rhodamine chemosensors based spirolactam derivatives RW1-3, which incorporate two kinds of phthlandione derivatives and two kinds of amino acids. They would be suitable for introducing O atom. However, O atom will provide even more binding sites that might be a choice to be parts of a selective receptor for the selective recognition of Hg^{2+} [42–44]. At the same time, we envisaged different phthlandione derivatives and amino acids can affect the fluorescence intensity of probes and the metal ion-selective recognition.

2. Experimental

2.1. Instruments

Fluorescence spectra were measured on a Hitachi F-4500 spectrofluorimeter with quartz cuvette (path length = 1 cm). The absorption spectra measurements were observed by a Purkinje General TU-1901 UV/Vis spectrometer. A pH-10C digital pH meter was utilized to measure the pH values of aqueous solutions. IR data were taken in KBr disks on TENSOR37 Fourier-Transform Infrared Spectrometer. ^{1}H NMR and ^{13}C NMR measurements were performed with a Varian Inova-400 MHz spectrometer with TMS as an internal standard and $CDCl_3$ as solvent. ESI-MS measurements were carried out on Waters QT of-Micro instrument.

2.2. Reagents

All reagents used were purchased from commercial suppliers and used without further purification. The solutions of metal ions were performed from their nitrate and chloride salts. Double-distilled water was used throughout the experiments. HEPES buffer solutions (10 mM, pH 7.0) were prepared in water.

2.3. Synthesis procedure

Synthesis of RW1 (Scheme 1): Rhodamine ethylenediamine was synthesized as reported method [45]. Phthalic anhydride (0.59 g, 4 mmol) and alanine (0.35 g, 4 mmol) were dissolved in dry toluene (20 mL), and the mixture were heated under reflux for 4 h; after removal of the toluene, the residue was dissolved in thionyl chloride (10 mL) and refluxed for 3 h. Rhodamine ethylenediamine (1.73 g, 4 mmol) was dissolved in dichloromethane (20 mL) in a 100 mL flask. An excess of triethylamine was added and dichloromethane (15 mL) solutions of 2-methylphthalimido acetyl chloride was added to this solution. The reaction mixture was stirred 2 h at 0–5 °C, after drying under reduced pressure, and pale yellow solid was observed. The target material was further purified by column chromatography with CH_3OH/CH_2Cl_2 (1:5 v/v) to give 1.5 g of **1** in 52% yield. ^{1}H NMR ($CDCl_3$, 400 MHz) δ = 7.95 (s, 1H), 7.90 (m, 2H), 7.79 (m, 2H), 7.29-7.40 (m, 3H), 7.05 (d, J = 7.2 Hz, 1H), 6.46 (d, J = 8.8 Hz, 1H), 6.32-6.38 (m, 4H), 6.27 (d, J = 8.4 Hz, 1H), 4.91(q, J = 7.2 Hz, 1H), 3.34 (m, 10H), 2.96 (m, 2H), 1.74 (t, J = 7.2 Hz, 3H), 1.17 (t, J = 6.8 Hz, 12H). ^{13}C NMR ($CDCl_3$, 100 MHz) δ = 168.93, 167.69, 154.12, 153.24, 153.07, 149.00, 148.93, 134.21, 132.70, 129.88, 128.49, 128.23, 128.06, 128.03, 123.39, 122.39, 108.31, 97.12, 64.72, 48.09, 43.68, 40.20, 38.35, 13.76, 11.59. IR (KBr, ν/cm^{-1}): 3425, 3003, 2856, 1673, 1612, 1460, 1224, 1118, 976. ESI-MS ($M + H^+$): m/z = 686.33. Anal. Calcd for $C_{41}H_{43}N_5O_5$: H, 6.32; C, 71.80; N, 10.21. Found: H, 6.25; C, 70.77; N, 10.16.

RW2 and RW3 were prepared with the similar synthetic method to RW1. Compound RW2: yield: 43%. ^{1}H NMR ($CDCl_3$, 400 MHz)

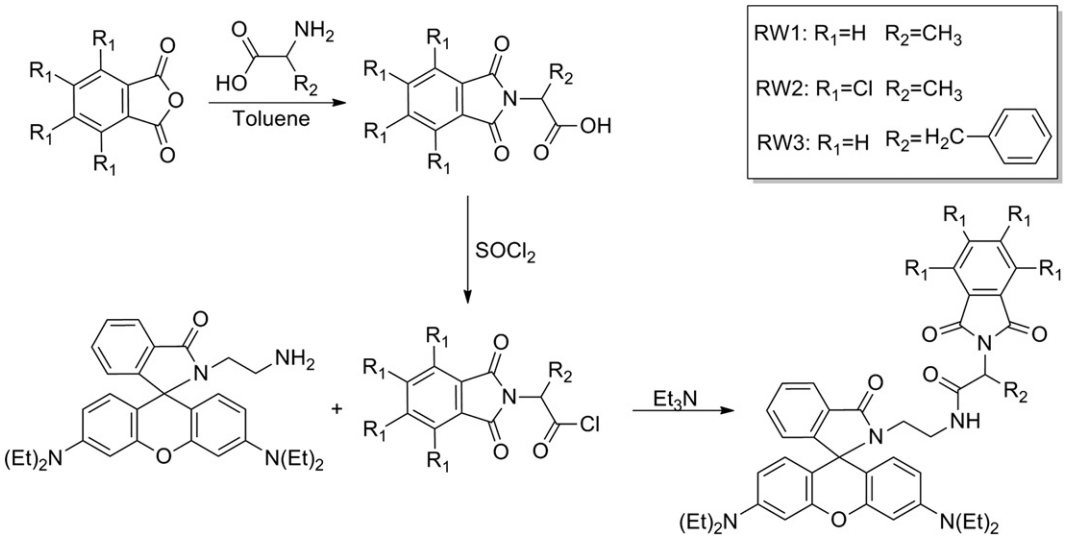

Scheme 1. Synthesis of RW1-3.

δ = 8.05 (s, 1H), 7.29–7.45 (m, 3H), 7.06 (d, J = 7.6 Hz, 1H), 6.26–6.45 (m, 6H), 4.91 (q, J = 7.2 Hz, 1H), 3.74 (q, J = 6.8 Hz, 1H), 3.36 (q, J = 7.2 Hz, 8H), 3.25 (m, 2H), 2.97 (d, J = 7.6 Hz, 1H), 1.73 (d, J = 7.2 Hz, 3H), 1.17 (t, J = 6.8 Hz, 12H). ^{13}C NMR ($CDCl_3$, 100 MHz) δ = 167.76, 153.98, 153.23, 152.99, 149.07, 148.90, 137.71, 132.83, 129.80, 129.17, 128.84, 128.01, 123.39, 122.51, 108.35, 104.52, 97.53, 65.17, 54.80, 44.14, 40.96, 38.48, 33.81, 12.14. IR (KBr, ν/cm^{-1}): 3426, 3004, 2858, 1673, 1615, 1457, 1220, 1112, 979. ESI-MS (M + H$^+$): m/z = 824.17. Anal. Calcd for $C_{41}H_{39}Cl_4N_5O_5$: H, 4.77; C, 59.79; N, 8.50. Found: H, 4.54; C, 58.89; N, 8.19.

Compound RW3: yield: 47%. ^{1}H NMR ($CDCl_3$, 400 MHz) δ = 7.95 (s, 1H), 7.89 (m, 4H), 7.79 (m, 4H), 7.28–7.42 (m, 4H),7.05 (d, J = 7.6 Hz, 1H), 6.27-6.46 (m, 6H), 4.92 (q, J = 7.6 Hz, 1H), 3.34 (m, 10H), 2.96 (t, J = 7.2 Hz, 2H), 1.74 (t, J = 6.8 Hz, 2H), 1.17 (q, J = 6.8 Hz, 12H). ^{13}C NMR ($CDCl_3$, 100 MHz) δ = 170.44, 167.41, 163.11, 153.84, 153.27, 153.04, 148.99, 139.84, 137.17, 132.90, 129.57, 128.72, 128.63, 128.47, 128.18, 128.03, 127.80, 126.74, 123.89, 122.18, 108.35, 104.23, 97.65, 65.88, 55.47, 44.35, 39.07, 33.73, 12.58. IR (KBr, ν/cm^{-1}): 3422, 3001, 2852, 1672, 1616, 1459, 1228, 1112, 974. ESI-MS (M + H$^+$): m/z = 762.36. Anal. Calcd for $C_{47}H_{47}N_5O_5$: H, 6.22; C, 74.09; N, 9.19. Found: H, 6.14; C, 72.93; N, 9.02.

2.4. Cell incubating imaging

Images of the human hepatocyte cell line (HL-7702 cells) were cultured in (Invitrogen) supplemented with 10% Fetal Bovine Serum (FBS, Invitrogen) in an atmosphere of 5% CO_2 at 37 °C. One day before imaging, cells were placed in 6-well flat-bottomed plates. Immediately, before the experiments, the HL-7702 cells were exposed to the probe RW1 (2.5×10^{-5} mol L^{-1}) for 30 min at room temperature to allow the probe to permeate into the cells and supplementing cells with 2.5×10^{-5} mol L^{-1} $Hg(ClO_4)_2$ in PBS at 37 °C under 5% CO_2 for another 30 min. The cells were washed with PBS three times and then imaged. The fluorescence imaging of intracellular was observed under an Olympus IX71 inverted fluorescence microscopy with 40 × objective lens (excited with green light). The HL-7702 cells only incubated with 10 μM RW1 for 30 min at 37 °C under 5% CO_2 was as a control.

3. Results and discussion

We take advantage was made of phthalic anhydride as an amino-protecting group, appropriate to introduce oxygen atoms, which are involved in the binding of metal ions. Then, due to the phthalimido acid chlorides possessing high reactivity, nucleophilic substitution can be prone to occur with rhodamine ethylenediamine.

3.1. Spectral characteristics

The binding behavior of RW1, RW2 and RW3 toward different cations, such as Ag^+, Ca^{2+}, Cd^{2+}, Co^{2+}, Al^{3+}, Cu^{2+}, Hg^{2+}, K^+, Pb^{2+}, Mg^{2+}, Mn^{2+}, Na^+, Ni^{2+}, Fe^{3+}, Au^+, Au^{3+} and Zn^{2+} ions were investigated by UV–vis and fluorescence spectroscopy. Among the various metal ions examined (10 equiv.), RW1 and RW2 showed highly selective "Off–On" absorption enhancement only with Hg^{2+} at methanol-H_2O (4:6, v/v, HEPES, pH 7.0) solution (Fig. 1). As shown, almost all the metal cations including the free RW1 and RW2 exhibit very little absorbance at 556 nm. However, Hg^{2+} resulted in a prominent change, which can be ascribed to the spirolactam bond cleavage followed by the formation of a delocalized xanthene moiety of the rhodamine group. Interestingly, Al^{3+} also yielded a significant absorption (Fig. 1a) enhancement with RW3 which contains the benzyl group at methanol-H_2O (4:6, v/v, HEPES, pH 7.0) solution. Upon the gradual addition of Al^{3+} up to 1 equiv., a new absorption band centered at 556 nm appeared with increasing intensity, accompanied by a clear color change from colorless to pink.

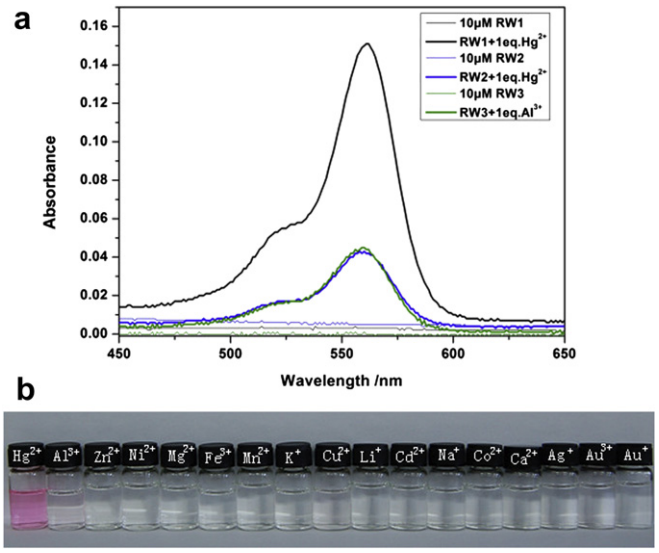

Fig. 1. (a) UV–vis absorption of RW1, RW2 and RW3 (10 μM) in 4:6 CH_3OH/HEPES buffer (v/v, 10 mM, pH 7.0) with 10 μM Hg^{2+} or Al^{3+}. (b) RW1 (10 μM) as a selective naked-eye chemosensor for Hg^{2+} (10 μM) in in 4:6 CH_3OH/HEPES buffer (v/v, 10 mM, pH 7.0).

In addition, the selectivity profiles of RW1, RW2 and RW3 for metal cations were investigated by fluorimetric experiments. The fluorescence spectra were obtained by excitation of the rhodamine fluorophore at 525 nm. Both a red color and the fluorescence characteristics of rhodamine B appear when upon the addition of Hg^{2+} to a colorless solution of RW1 and RW2 (Fig. 2a). In the presence of other metal ions, such as alkali and alkaline earth metal ions (K^+, Na^+, Mg^{2+}, Ca^{2+}) and other transition metal ions (Mn^{2+}, Ni^{2+}, Co^{2+}, Cu^{2+}, Zn^{2+}, Cd^{2+}, Ag^+, Pb^{2+}, Al^{3+}, Fe^{3+}, Au^+, Au^{3+}), there were no evident fluorescence intensity enhancement (Fig. 2b). Apparently, due to Hg^{2+}-induced significant fluorescence enhancement, Hg^{2+} could be distinguished from other metal ions. RW3 showed only a very weak fluorescence in the absence of metal ions. The addition of Al^{3+} resulted in remarkably enhanced fluorescence intensity. Under the same condition, additions of other metal ions including K^+, Na^+, Mg^{2+}, Ca^{2+}, Mn^{2+}, Ni^{2+}, Co^{2+}, Cu^{2+}, Zn^{2+}, Cd^{2+}, Ag^+, Pb^{2+}, Al^{3+}, Fe^{3+}, Au^+ and Au^{3+} did not cause any discernible changes. Since the C–C π bonds of the benzene ring disappear due to the presence of Al^{3+}. Each of the resulting singly occupied carbon p-orbitals interacts with two of the three empty 3p-orbitals of aluminum (the ones parallel to the aromatic ring plane). Each σ C–C bond also interacts with the Al^{3+} empty 3s-orbital, and the remaining 3p-orbital [46]. The bonding orbitals formed by the 5d orbitals of Hg^{2+} are completely filled, resulting in a closed-shell electronic configuration. So the benzene rings of RW3 have better selectivity of electron-deficient Al^{3+} ($3s^0\ 3p^0$) than completely fill 5d orbitals Hg^{2+} ($5d^{10}\ 6s^0$).

Achieving high selectivity toward the sensors over the other competitive species coexisting in the sample is a very important feature to evaluate the performance of a fluorescence chemosensor. In certain environmental samples, such as river and seawater, the concentrations of some prevalent toxic metal ions are significantly higher, therefore competition experiments with high concentrations of the above-mentioned metal ions (10 equiv.) were carried

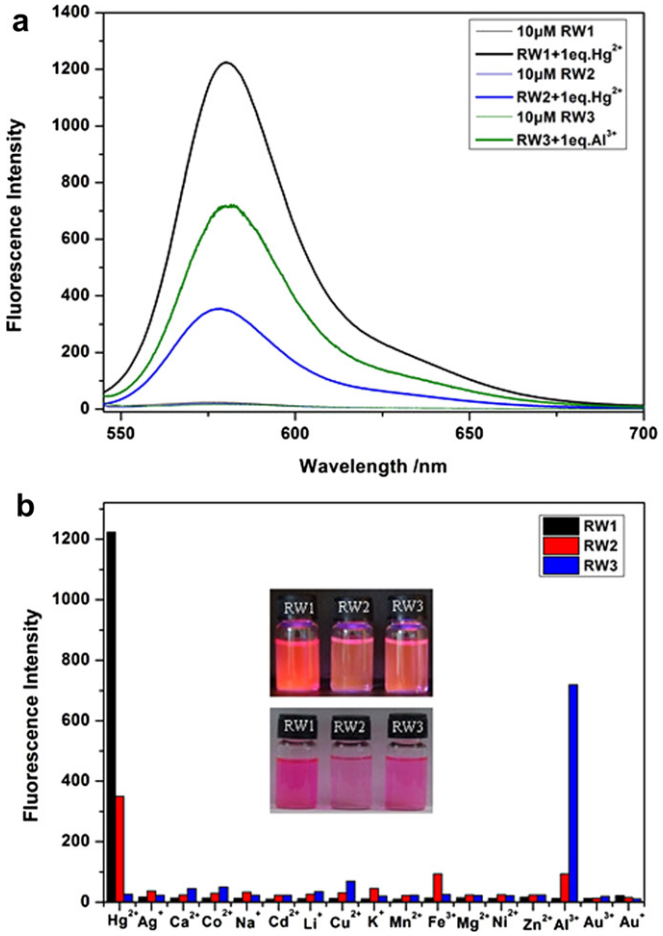

Fig. 2. (a) Fluorescent spectra of RW1, RW2 and RW3 (10 μM) in 4:6 CH_3OH/HEPES buffer (v/v, 10 mM, pH 7.0) with 10 μM Hg^{2+} or Al^{3+}. (b) Fluorescence responses of RW1, RW2 and RW3 (10 μM) to various cations (25 mM) at 581 nm in 4:6 CH_3OH/HEPES buffer (v/v, 10 mM, pH 7.0). Inset: Pictures of RW1, RW2 and RW3 as a selective naked-eye chemosensors (bottom) and the visual fluorescence emissions by using a UV lamp (365 nm) (top) for Hg^{2+} or Al^{3+}.

out. The competition experiments revealed that the Hg^{2+}/Al^{3+}-induced fluorescence response was unaffected in by 10 equiv. of environmentally relevant alkali or alkaline-earth metals, such as Na^+, K^+, Mg^{2+} and Ca^{2+}. In addition, the other transition metal ions (Mn^{2+}, Ni^{2+}, Co^{2+}, Cu^{2+}, Zn^{2+}, Cd^{2+}, Ag^+, Pb^{2+}, Al^{3+}, Fe^{3+}, Au^+, Au^{3+}) did not interfere with the Hg^{2+}/Al^{3+}-induced fluorescence (Fig. 3). Obviously, all of these results confirmed that our proposed chemosensor RW1-2/RW3 has remarkably high selectivity toward Hg^{2+}/Al^{3+} ions over other competitive cations in the water medium.

Figs. 4 and 5 explain the fluorescent and absorption titrations of RW1 and RW2 with Hg^{2+} in methanol-H_2O (4:6, v/v, 10 mM, HEPES, pH 7.0) solution. On addition of Hg^{2+} ions (1–20 μM), the solution of RW1 and RW2 turned from colorless to pink, and the absorbance was significantly enhanced with a new peak appearing at around 556 nm (Fig. 4), clearly suggesting the formation of the ring-opened form of RW1 and RW2 as a result of Hg^{2+} binding. Compared to RW1, the enhancement in the UV absorption (λ_{max} = 556 nm) of RW2 from 180 fold under to 60 fold.

To understand the recognition abilities of RW1-2/RW3 toward Hg^{2+}/Al^{3+} ions, the Job's plot analysis for the absorbance was conducted to determine the binding stoichiometry of the RW1-2/RW3 and Hg^{2+}/Al^{3+} ions complex, by according to the continuous variations with a total concentration of [Hg^{2+}/Al^{3+}] + [RW1-2/RW3] of 20 μM and changing the mole fraction of Hg^{2+}/Al^{3+} ions from 0 to 1 (Fig. 4, inset). From the Job's plot, the absorbance of RW1-2/RW3 approached a maximum when the molar fraction of Hg^{2+}/Al^{3+} was 0.5, indicating a 1:1 stoichiometry was most possible for the binding mode of the RW1-2/RW3 and Hg^{2+}/Al^{3+}.

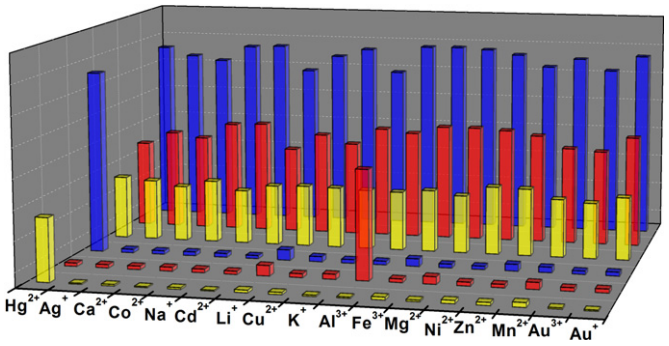

Fig. 3. Fluorescent intensity of RW1 (bule bars), RW2 (yellow bars) and RW3 (red bars) (10 μM) to various cations in 4:6 CH_3OH/HEPES buffer (v/v, 10 mM, pH 7.0). The front 3 bars represent the emission intensities of RW1, RW2 and RW3 in the presence of other cations (10 equiv.), respectively. The back 3 bars represent the emission intensities that occur upon the subsequent addition of 10 μM of Hg^{2+} or Al^{3+} to the above solution, respectively. (λ_{ex} = 525 nm, λ_{em} = 581 nm). (For interpretation of the references to colour in this figure legend, the reader is referred to the web version of this article.)

The complexation of Hg^{2+} by RW1 and RW2 were also investigated by means of fluorescence titration in methanol-H_2O (4:6, v/v, HEPES, pH 7.0) solution. Addition of increasing concentrations of Hg^{2+} ions to the solutions of RW1 (Fig. 5a) and RW2 (Fig. 5b) resulted in the gradual increase of the fluorescence intensity with emission peak at 581 nm, reaching saturation at addition of 1.5 equiv. Hg^{2+}. Nonlinear least-squares fitting of the titration profiles based on the 1:1 binding model strongly support the 1:1 stoichiometry of RW1 (Fig. 5a, inset) and RW2 (Fig. 5b, inset) with Hg^{2+}, and the binding constant was calculated to be 2.1 × 10^7 and 4.4 × 10^5, Respectively [47]. The equation used was:

$$Y = Y_0 + \frac{Y_{\lim} - Y_0}{2}\left\{1 + \frac{C_M}{C_L} + \frac{1}{K_S C_L} - \left[\left(1 + \frac{C_M}{C_L} + \frac{1}{K_S C_L}\right)^2 - 4\frac{C_M}{C_L}\right]^{1/2}\right\},$$

where Y is the recorded fluorescent intensity, Y_0 is the start value without addition of ions, Y_{lim} is the limiting value, C_M is the ions concentration, and C_L is the sensor concentration.

The above results indicate that the sensor RW1 exhibited a superior binding capability toward the Hg^{2+} ions relative to the sensor RW2, which can be attributed to additional chloride atoms in the case of RW2. This observation along with lower binding constant of RW2 suggests that the chloride atom plays an important role in the extent of the binding with Hg^{2+}. The chlorine atom led to the heavy atom effect and the electrophilic effect which can lead to a decrease in fluorescence intensity [48].

To gain more insight into the properties and mechanism of RW3 toward Al^{3+}, fluorescence titration with Al^{3+} was recorded. As seen from Fig. 5c, upon sequential addition of Al^{3+}, an emission band peaked at 581 nm significantly increased in fluorescence intensity, possibly because of the rhodamine ring-opening process, and the fluorescence intensity increased up to 1.3 equiv. and then no changes were observed up to 2.0 equiv. Based on 1:1 stoichiometric relationship, a binding constant of 3.9 × 10^5 M^{-1} was obtained from

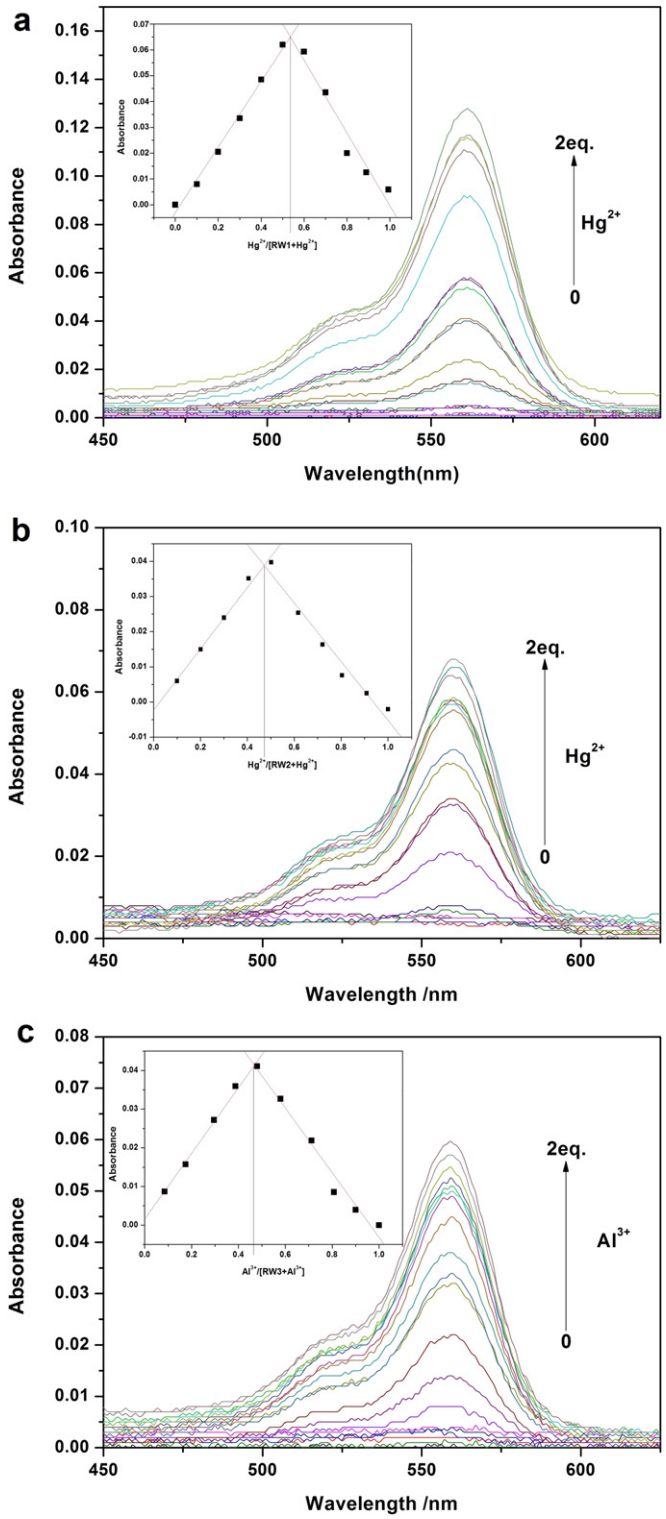

Fig. 4. Absorption spectra of RW1 (a), RW2 (b) and RW3 (c) (10 mM) in 4:6 CH_3OH/HEPES buffer (v/v, 10 mM, pH 7.0) upon addition of different amounts of Hg^{2+} and Al^{3+} ions (0–2 equiv.). Inset: Job's plots at 556 nm (RW1, RW2 and RW3).

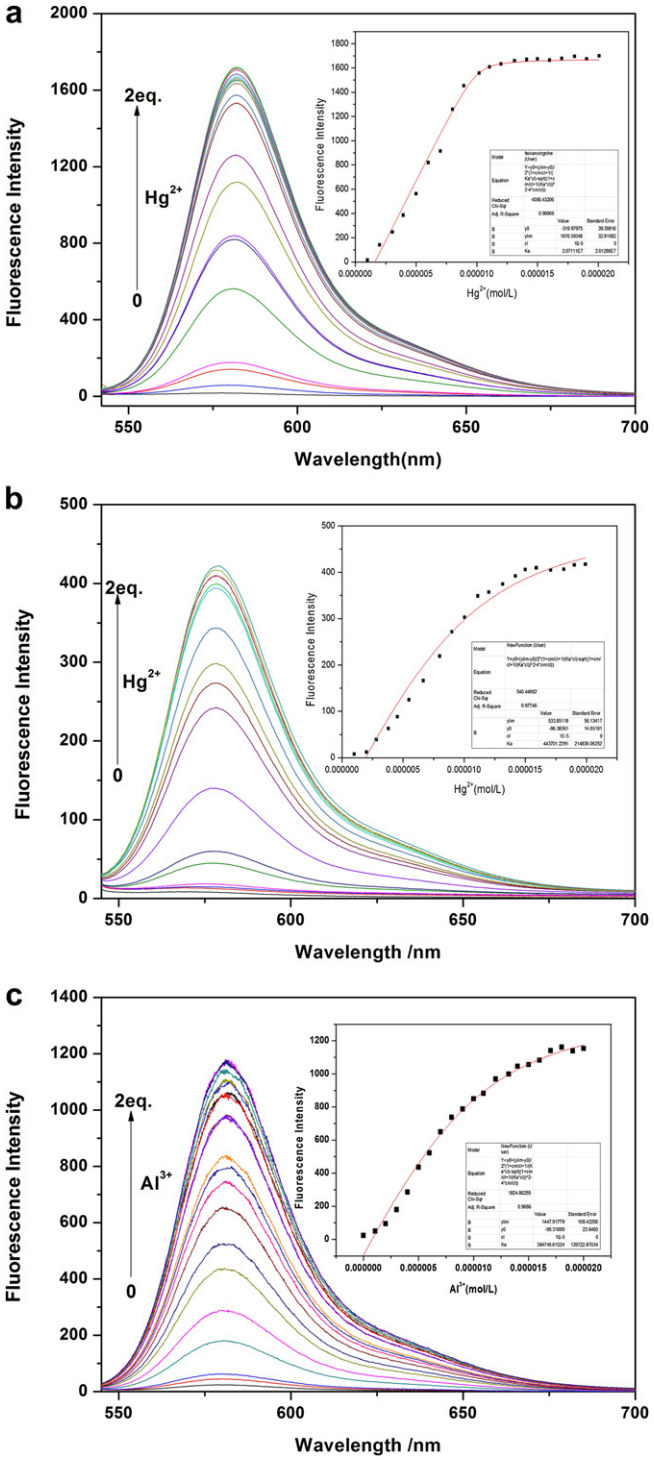

Fig. 5. Fluorescence spectra of RW1 (a), RW2 (b) and RW3 (c) (10 mM) in 4:6 CH_3OH/HEPES buffer (v/v, 10 mM, pH 7.0) upon addition of different amounts of Hg^{2+} and Al^{3+} ions (0–2 equiv.). λ_{ex} = 525 nm. Inset: Top: Fluorescence at 581 nm as a function of Hg^{2+} and Al^{3+} concentration, indicating a 1:1 metal-ligand ratio; bottom: Fluorescence intensity at 581 nm for RW1, RW2, and RW3 as a function of the concentration of Hg^{2+} ion.

a nonlinear least-squares fit according to a 1:1 binding stoichiometry (Fig. 5c, inset).

The high sensitivity of RW1-2/RW3 for Hg^{2+}/Al^{3+} ions might be used to generate a calibration curve for quantitative measurement of Hg^{2+}/Al^{3+} ions in aqueous solution. By adding Hg^{2+}/Al^{3+} ions with different concentrations ranged from 0 to 10 μM, the fluorescence intensity of RW1-2/RW3 at 581 nm was recorded to generate a calibration curve. When Hg^{2+} concentration added was from 0.5 to 10 μM, an almost perfect linearity was found between fluorescence intensity of RW1-2/RW3 and

Hg^{2+}/Al^{3+} concentration (Supporting data, Figs. S1–S3). The limit of detection (LOD) was attained of 2.5×10^{-8} M, 4.2×10^{-8} M and 2.9×10^{-8} M, respectively, based on $3 \times \delta_{blank}/k$ (where δ_{blank} is the standard deviation of the blank solution and k is the slope of the calibration plot). The results indicated that the RW1-2/RW3 chemosensor could sensitively detect environmentally relevant levels of Hg^{2+}/Al^{3+}.

3.2. pH investigation

To apply the probe in complex environments, the stabilities of the two probes were tested in the absence and presence of Hg^{2+} at different pH values. Fig. 6 shows that for free RW1 in the pH range of 3.0–4.0, the emission increased as the pH decreased the ring-opening of the rhodamine framework took place due to the strong protonation. When pH > 4.0, It can be seen that the fluorescence was of very low intensity and indicating no significant ring-opening. However, after the addition of Hg^{2+}, the emission increased substantially between pH 4.0 and 8.0. Thus, RW1 can detect Hg^{2+} ions with a wide pH range (4.0–8.0) because in this region RW1 with Hg^{2+} induces a remarkable fluorescence "Off–On", whereas RW1 without Hg^{2+} does not lead to such change. Under identical condition, RW2 and RW3 show similar behavior. In the pH range from 5.0 to 8.0, RW1-2/RW3 can respond to Hg^{2+}/Al^{3+} without any interference by protons.

3.3. Theoretical mechanism

Thus, in accordance with the 1:1 stoichiometry, the sensors are the most likely to be chelated with metal ions via its O atoms (Fig. 7, inset) [49,50]. On the other hand, reversibility of target ion binding is an important quality in a probe. Consequently, we also investigated the reversibility of the RW1 and RW2-Hg^{2+} binding by a simple titration methodology with Na_2S. Na_2S was introduced because of its sulfide ion has a strong binding ability toward thiophilic Hg^{2+}. Addition of Na_2S to the RW1 and RW2-Hg^{2+} complex led to an expected decrease of fluorescence intensity (Fig. 7). The solution returned to its original colorless state, which reveals that the reversibility due to the chelation-induced ring opening of rhodamine spirolactam, rather than other possible reactions.

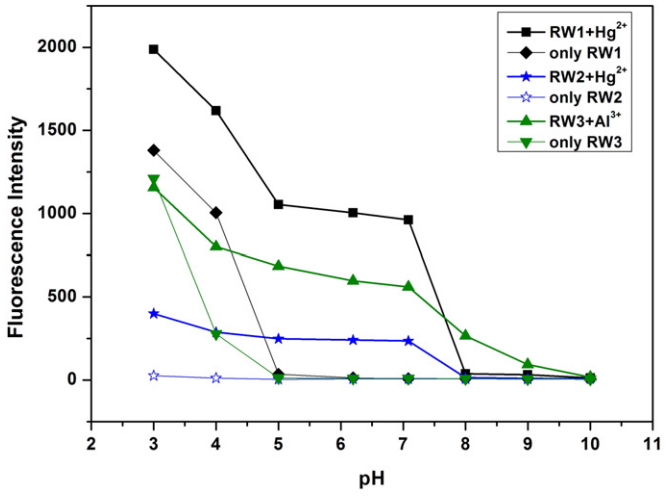

Fig. 6. Fluorescence intensity (581 nm) of RW1 RW2 and RW3 (10 μmol L^{-1}) in 4:6 CH_3OH/HEPES buffer (v/v, 10 mM, pH 7.0) of different pH in the absence and presence of Hg^{2+} or Al^{3+} (10 μmol L^{-1}).

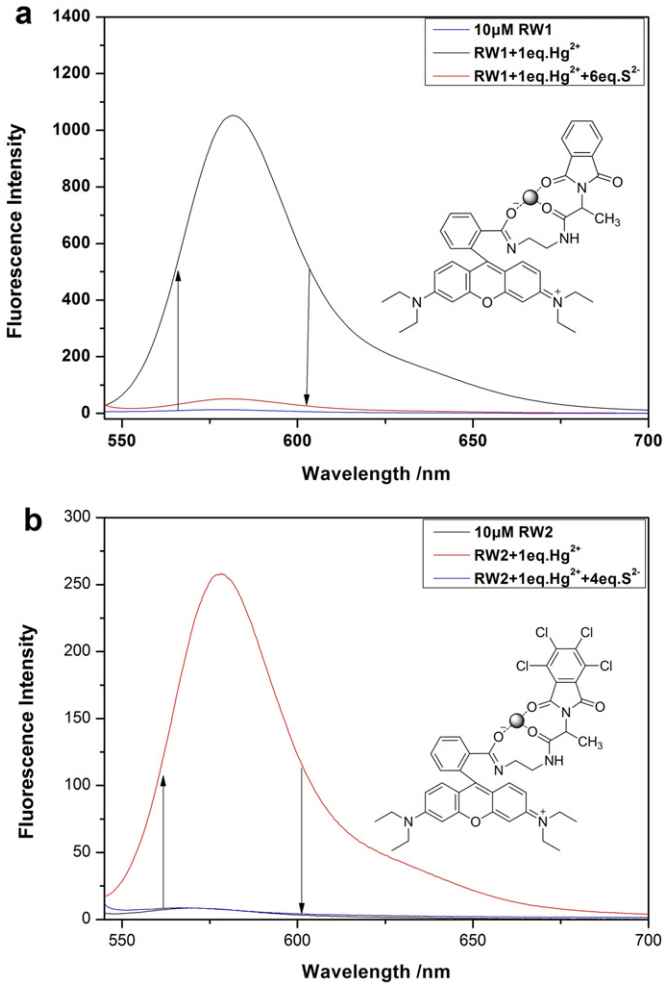

Fig. 7. Reversible investigation of RW1 and RW2 for Hg^{2+} with addition of S^{2-}.

IR titration results clearly supported the proposed ring-opening mechanism. As demonstrated in Fig. S4 (Supporting data), the carbonyl absorption of RW1 at 1670 cm^{-1} shifted to a lower frequency at 1633 cm^{-1} upon the addition of Hg^{2+}, indicating that the carbonyl oxygen coordinated with Hg^{2+} resulting in the spirocycle ring opening. A similar behavior was observed for RW2 and RW3, as shown in Fig. S4 (Supporting data).

The ^{13}C NMR spectra of RW1-3 recorded in the absence or presence Hg^{2+}/Al^{3+} ions clearly show the involvement of carbonyl oxygen of RW1-3 in complex formation. The reduction in the ^{13}C-resonance at near 65 ppm confirms the opening of spirolactam ring upon complex formation with Hg^{2+}/Al^{3+} ions [51] (Supporting data, Figs. S5–S10).

3.4. Preliminary analytical application

In view of the above-mentioned advantages of the sensor RW1, bioimaging applications of RW1 for monitoring of Hg^{2+} ions in living cells were then carried out. After HL-7702 cells were incubated with RW1 (10 μM) in culture medium for 30 min at 37 °C, and no fluorescence of RW1 inside the living HL-7702 cells was observed (Fig. 8b). After three times washing with PBS buffer, The cells were then supplemented with 10 μM $Hg(NO_3)_2$ in the growth medium for another 30 min at 37 °C, a

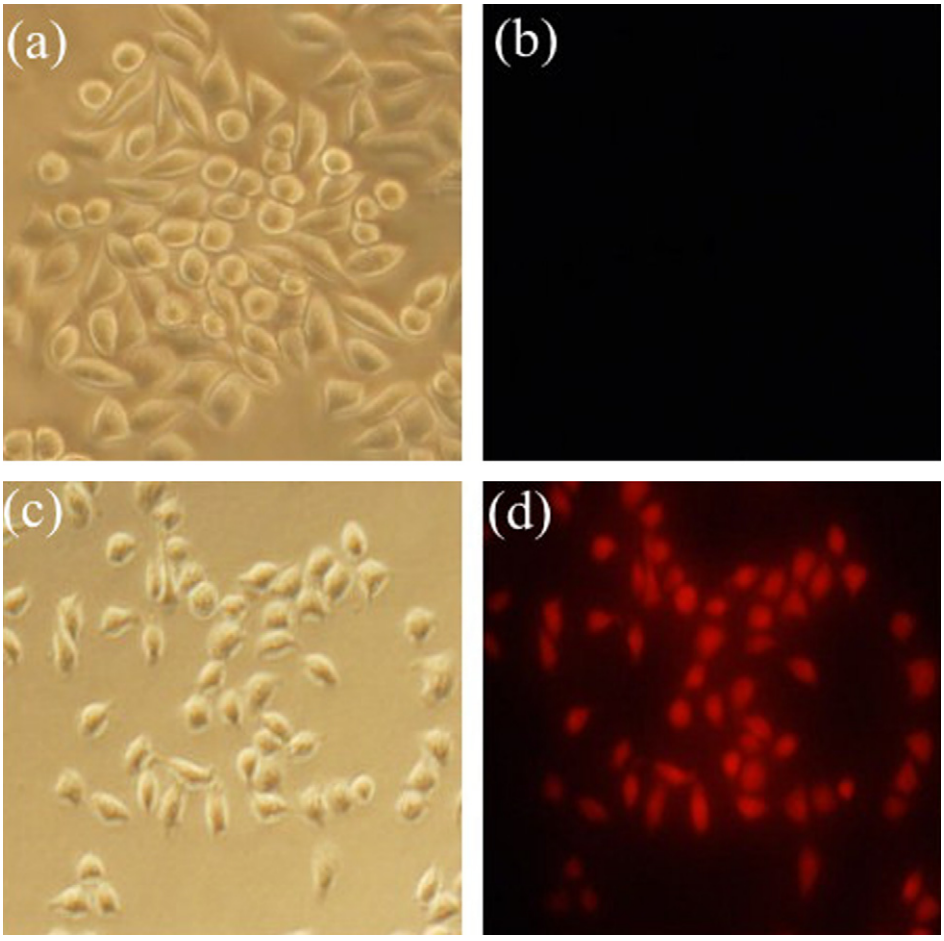

Fig. 8. Fluorescence images of Hg^{2+} in HL-7702 cells with 10 μM solution of RW1 in ethanol-PBS (1:99, v/v) buffer for 30 min at 37 °C, bright-field transmission image (a and c) and fluorescence image (b and d) of HL-7702 cells incubated with 0 μM, 10 μM of Hg^{2+} for 30 min, respectively.

bright fluorescence was observed from within the cell (Fig. 8d). A bright-field transmission image of cells treated with RW1 and Hg^{2+} confirmed that the cells were viable throughout the imaging experiments (Fig. 8a, c). It is proven that RW1 is cell-permeable and primarily little toxic to the cell culture. These results demonstrated that RW1 may be used for detecting Hg^{2+} in biological samples. The fluorescence imaging experiments of RW2 and RW3 are shown in the supporting information (Figs. S11–S12) [50,52–66].

To evaluate cytotoxicity of RW1 was taken as an example to perform a assay on HL-7702 cells with dye concentrations from 0 to 10 μM. A cytotoxicity screen (Fig. 9) was conducted for four dye concentrations: 0 μM, 0.1 μM, 1 μM, 10 μM. The cellular viability estimated was ca. 97% in 24 h after treatment with 10 μM of RW1, exhibiting low toxicity to HL-7702 cells.

3.5. Method performance comparison

Table 1 summarizes the performance of typical Hg^{2+} fluorescent chemosensors and highlights their applications. Most of the probes present coordination mode was 1:1 with Hg^{2+} [67,68,70,72–77]. Although all the probes have good selectivity for Hg^{2+}, a few of probes possess a wide quantitative range [68,70,72,74,75,78], even down to nM LOD [72,74,75]. However some of the probes require more rigorous testing media [68,69,71], and the reproductivity [68–70,72,73,75–77] as well as the applicability in living cells [67,68,72–74,76–78], are investigated. RW1 based on rhodamine shows a number of attractive characteristics such as good selectivity, high sensitivity and wide applicability. RW1 can be used for rapid analysis of trace level Hg^{2+} in living cells with satisfactory results.

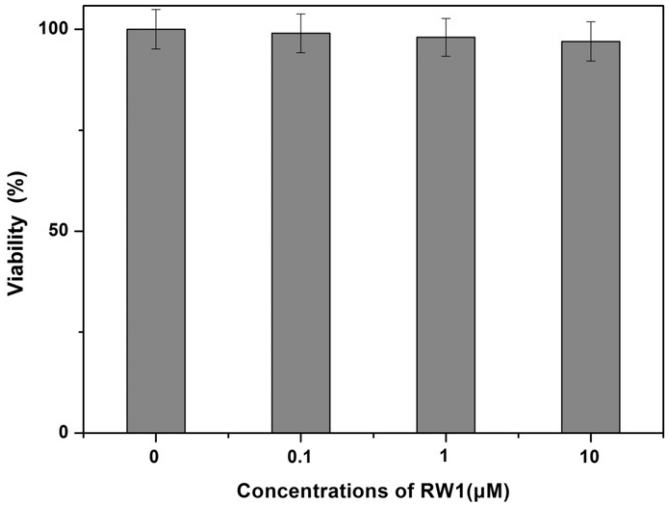

Fig. 9. Cell viability values (%) estimated by MTT proliferation test versus incubation concentrations of RW1. HL-7702 cells were cultured in the presence of 0–10 μM RW1 at 37 °C.

Table 1
Performances comparison of various "Off–On" probes for Hg^{2+}.

Reagents	Linear range, μM	LOD,nM	Coordination mode (probe:ion)	Testing media	Applications	Reproducibility	Ref.
Rhodamine derivative	NA[a]	NA	1:1	Water/CH_3CN(1:1, v/v pH = 7 NaAc–HAc)	Rat Schwann cells	NA	[67]
Rhodamine derivative	0–25	80	1:1	100% CH_3CN	Hela cells	Reversible	[68]
Rhodamine derivative	NA	500	1:2	100% THF	NA	Reversible	[69]
Rhodamine derivative	0.08–10	40	1:1	Water/ethanol (1:1, v/v pH = 7.24 Tris–HCl)	NA	Reversible	[70]
BINOL derivative	NA	NA	1:2	100% CH_3CN	NA	NA	[71]
Rhodamine derivative	0–0.35	8.25	1:1	Methanol–HEPES buffer (30:70, v/v, 20 mM HEPES, pH 7.0)	HL-7702 cells	Reversible	[72]
Rhodamine derivative	NA	NA	1:1	CH_3CN–H_2O (4:1, v/v; 10 μM tris HCl buffer; pH = 7.0)	HeLa cells	Reversible	[73]
Rhodamine derivative	1–28	1.41	1:1	1:99 ethanol/H_2O (v/v, pH 7.0)	K 562 cells	NA	[74]
1,8-anthrancene disulfonamide	0.2–2	0.79	1:1	Water containing 2% (v/v) of DMSO	NA	Reversible	[75]
Rhodamine derivative	NA	NA	1:1	20 mM, MeCN–water solution, 95:5,v/v, pH = 7.2)	HeLa cells	Reversible	[76]
Rhodamine derivative	NA	NA	1:1	1×10^{-2} mol L^{-1} HEPES, 1×10^{-1} M $NaClO_4$, pH = 7.4, 50% ethanol, v/v)	A549 cells	Reversible	[77]
Rhodamine derivative	0.1–1	100	2:1	Water–DMF solution (1/1, v/v, pH = 7.0 NaAc–HAc)	Rat Schwann cells	Reversible	[78]
Rhodamine derivative	0.1–3	25	1:1	CH_3OH/HEPES buffer (4:6, v/v, 10 mM, pH 7.0)		Reversible	This work of RW1

[a] Na: Not available.

4. Conclusion

In conclusion, rhodamine derivatives RW1-2/RW3 were synthesized by the one-step condensation between Rhodamine ethylenediamine with phthalimido acid chlorides and behave as selective fluorescent and colorimetric sensors for Hg^{2+}/Al^{3+} in aqueous solution. Complexation of the Hg^{2+}/Al^{3+} ions open the spirolactam ring of rhodamine moieties to give specific color change as well as fluorescence enhancement at 581 nm. Most importantly, due to the presence of chlorine atoms, RW2 has a lower binding constant than RW1 for the Hg^{2+}. In addition, Moreover, the benzyl group can make RW3 better identify Al^{3+}. The living cell imaging experiments further demonstrate the value of RW1-3 in the practical applications in biological systems.

Acknowledgments

The authors thank the financial supports from the National Natural Science Foundation of China (50973084), Science and Technical Development Foundation of Colleges and Universities, Tianjin, China (20071214).

Appendix A. Supplementary data

Supplementary data related to this article can be found at http://dx.doi.org/10.1016/j.dyepig.2013.02.002.

References

[1] Cai GB, Zhao GX, Wang XK, Yu SH. Synthesis of polyacrylic acid stabilized amorphous calcium carbonate nanoparticles and their application for removal of toxic heavy metal ions in water. J Phys Chem C 2010;114:12948–54.
[2] Thirumavalavan M, Lai YL, Lin LC, Lee JF. Cellulose-based native and surface modified fruit peels for the adsorption of heavy metal ions from aqueous solution: langmuir adsorption isotherms. J Chem Eng Data 2010;55:1186–92.
[3] Zhuang Y, Yang Y, Xiang GL, Wang X. Magnesium silicate hollow nanostructures as highly efficient absorbents for toxic metal ions. J Phys Chem C 2009;113:10441–5.
[4] Tavakoli O, Yoshida H. Effective recovery of harmful metal ions from squid wastes using subcritical and supercritical water treatments. Environ Sci Technol 2005;39:2357–63.
[5] Cheng HF, Hu YA. China needs to control mercury emissions from municipal solid waste (MSW) incineration. Environ Sci Technol 2010;44:7994–5.
[6] Fan J, Guo K, Peng XJ, Du JJ, Wang JY, Sun SG, et al. A Hg^{2+} fluorescent chemosensor without interference from anions and Hg^{2+}-imaging in living cells. Sens Actuators B 2009;142:191–6.
[7] Cheng HF, Hu YA. Understanding the paradox of mercury pollution in China: high concentrations in environmental matrix yet low levels in fish on the market. Environ Sci Technol 2012;46:4695–6.
[8] Liu YW, Chen CH, Wu AT. A turn-on and reversible fluorescence sensor for Al^{3+} ion. Analyst 2012;137:5201–3.
[9] Weller DG, Gutierrez AJ, Rubio C, Revert C, Hardisson A. Dietary intake of aluminum in a Spanish population (Canary islands). J Agr Food Chem 2010;58:10452–7.
[10] Ruan JJ, Xu ZM. Approaches to improve separation efficiency of eddy current separation for recovering aluminum from waste toner cartridges. Environ Sci Technol 2012;46:6214–21.
[11] Dockery CR, Blew MJ, Goode SR. Visualizing the solute vaporization interference in flame atomic absorption spectroscopy. J Chem Educ 2008;85:854.
[12] Almeida ILS, Coelho NMM. Direct determination of inorganic mercury in ethanol fuel by cold vapor atomic absorption spectrometry. Energ Fuels 2012;26:6003–7.
[13] Gonzalez PR, Epov VN, Bridou R, Tessier E, Guyoneaud R, Monperrus M, et al. Species-specific stable isotope fractionation of mercury during Hg(II) methylation by an anaerobic bacteria (Desulfobulbus propionicus) under dark conditions. Environ Sci Technol 2009;43:9183–8.
[14] Roy V, Amyot M, Carignan R. Beaver ponds increase methylmercury concentrations in Canadian shield streams along vegetation and pond-age gradients. Environ Sci Technol 2009;43:5605–11.
[15] Chen XQ, Baek KH, Kim Y, Kim SJ, Shin I, Yoon J. A selenolactone-based fluorescent chemodosimeter to monitor mecury/methylmercury species in vitro and in vivo. Tetrahedron 2010;66:4016–21.
[16] Lohani CR, Kim JM, Chung SY, Yoon JY, Lee KH. Colorimetric and fluorescent sensing of pyrophosphate in 100% aqueous solution by a system comprised of rhodamine B compound and Al^{3+} complex. Analyst 2010;135:2079–84.
[17] Maity DR, Daraju TG. Conformationally constrained (Coumarin-Triazolyl-Bipyridyl) click fluoroionophore as a selective Al^{3+} sensor. Inorg Chem 2010;49:7229–31.
[18] Kang J, Zhang YM, Huang ZX, Han L. Directly oxidized chemiluminescence of 2-Substituted-4,5-di(2-Furyl)-1H-imidazole by acidic potassium permanganate and its analytical application for determination of albumin. J Fluoresc 2011;21:1607–15.
[19] Jung JY, Han SJ, Chun J, Lee C, Yoon J. New thiazolothiazole derivatives as fluorescent chemosensors for Cr^{3+} and Al^{3+}. Dyes Pigm 2012;94:423–6.
[20] Sun X, Wang YW, Peng Y. A selective and ratiometric bifunctional fluorescent probe for Al^{3+} ion and proton. Org Lett 2012;14:3420–3.
[21] Zhou Y, You XY, Fang Y, Li JY, Liu K, Yao C. A thiophen-thiooxorhodamine conjugate fluorescent probe for detecting mercury in aqueous media and living cells. Org Biomol Chem 2010;8:4819–22.
[22] Huang JH, Xu YF, Qian XH. A rhodamine-based Hg^{2+} sensor with high selectivity and sensitivity in aqueous solution: a NS2-containing receptor. J Org Chem 2009;74:2167–70.

[23] Liu K, Zhou Y, Yao C. A highly sensitive and selective ratiometric and colorimetric sensor for Hg^{2+} based on a rhodamine–nitrobenzoxadiazole conjugate. Inorg Chem Commun 2011;14:1798–801.
[24] Drummond MJ, Fry CS, Glynn EL, Timmerman KL, Dickinson JM, Walker DK, et al. Skeletal muscle amino acid transporter expression is increased in young and older adults following resistance exercise. J Appl Physiol 2010; 111:135–42.
[25] Melone M, Varoqui H, Erickson JD, Conti F. Localization of the Na^{+}-coupled neutral amino acid transporter 2 in the cerebral cortex. Neuroscience 2006; 140:281–92.
[26] Yang HM, Park CW, Ahn T, Jung B, Seo BK, Park JH, et al. A direct surface modification of iron oxide nanoparticles with various poly(amino acid)s for use as magnetic resonance probes. J Colloid Interf Sci 2012;391:158–67.
[27] Vesely T, Trakal L, Neuberg M, Szakova J, Drabek O, Tejnecky V, et al. Removal of Al, Fe and Mn by Pistia stratiotes L. and its stress response. Cent Eur J Biol 2012;7:1037–45.
[28] Liu XH, Li JS, Dong JS, Hu C, Gong WM, Wang JY. Genetic incorporation of a metal-chelating amino acid as a probe for protein electron transfer. Angew Chem Int Edit 2012;51:10261–5.
[29] Park N, Ryu J, Jang S, Lee HS. Metal ion affinity purification of proteins by genetically incorporating metal-chelating amino acids. Tetrahedron 2012;68: 4649–54.
[30] Kwon SK, Kim HN, Rho JH, Swamy KMK, Shanthakumar SM, Yoon J. Rhodamine derivative bearing histidine binding site as a fluorescent chemosensor for Hg^{2+}. Bull Korean Chem Soc 2009;30:719–21.
[31] Xiang Y, Tong AJ, Jin PY, Ju Y. New fluorescent rhodamine hydrazone chemosensor for Cu (II) with high selectivity and sensitivity. Org Lett 2006;8: 2863–6.
[32] Huang W, Song C, He C, Lv G, Hu X, Zhu X, et al. Recognition preference of rhodamine-thio spirolactams for mercury (II) in aqueous solution. Inorg Chem 2009;48:5061–72.
[33] Kwon JY, Jang YJ, Lee YJ, Kim KM, Yoon J. A highly selective fluorescent chemosensor for Pb^{2+}. J Am Chem Soc 2005;127:10107–11.
[34] Yu CW, Chen LX, Zhang J, Li JH, Liu P, Wang WH, et al. "Off–On" based fluorescent chemosensor for Cu^{2+} in aqueous media and living cells. Talanta 2011;85:1627–33.
[35] Huang L, Wang X, Xie GQ, Xi PX, Li ZP, Xu M, et al. A new rhodamine-based chemosensor for Cu^{2+} and the study of its behavior in living cells. Dalton Trans 2010;39:7894–6.
[36] Dong L, Wu C, Zeng X, Mu L, Xue SF, Tao Z, et al. The synthesis of a rhodamine B schiff-base chemosensor and recognition properties for Fe^{3+} in neutral ethanol aqueous solution. Sens Actuators B 2010;145:433–7.
[37] Tang LJ, Li FF, Liu MH, Nandhakumar R. Single sensor for two metal ions: colorimetric recognition of Cu^{2+} and fluorescent recognition of Hg^{2+}. Spectrochim Acta A 2011;78:1168–72.
[38] Kim HN, Ren WX, Kim JS, Yoon J. Fluorescent and colorimetric sensors for detection of lead, cadmium, and mercury ions. Chem Soc Rev 2012;41:3210–44.
[39] Chen XQ, Pradhan T, Wang F, Kim JS, Yoon J. Fluorescent chemosensors based on spiroring-opening of xanthenes and related derivatives. Chem Rev 2012; 112:1910–56.
[40] Ding JH, Yuan LD, Gao L, Chen JW. Fluorescence quenching of a rhodamine derivative: selectively sensing Cu^{2+} in acidic aqueous media. J Lumin 2012; 132:1987–93.
[41] Yan FY, Cao DL, Wang M, Yang N, Yu QH, Dai LF, et al. A new rhodamine-based "Off–On" fluorescent chemosensor for Hg (II) ion and its application in imaging Hg (II) in living cells. J Fluoresc 2012;22:1249–56.
[42] Chen XQ, Jou MJ, Lee H, Kou S, Lim J, Nam SW, et al. New fluorescent and colorimetric chemosensors bearing rhodamine and binaphthyl groups for the detection of Cu^{2+}. Sens Actuators B 2009;137:597–602.
[43] Zheng XY, Zhang WJ, Mu L, Zeng X, Xue SF, Tao Z, et al. A novel rhodamine-based thiacalix[4]arene fluorescent sensor for Fe^{3+} and Cr^{3+}. J Incl Phenom Macro 2010;68:139–46.
[44] Soh JH, Swamy KMK, Kim SK, Kim S, Lee SH, Yoon J. Rhodamine urea derivatives as fluorescent chemosensors for Hg^{2+}. Tetrahedron Lett 2007;48: 5966–9.
[45] Zhang X, Shiraishi Y, Hirai T. Cu (II) selective green fluorescence of a rhodamine-diacetic acid conjugate. Org Lett 2007;9:5039–42.
[46] Mercero JM, Matxain JM, Lopez X, Fowler JE, Ugalde JM. Aluminum (III) interactions with the side chains of aromatic aminoacids. Int J Quantum Chem 2002;90:859–81.
[47] Tang LJ, Li Y, Nandhakumar R, Qian JH. An unprecedented rhodamine-based fluorescent and colorimetric chemosensor for Fe^{3+} in aqueous media. Monatsh Chem 2010;141:615–20.
[48] Romanova Zinaida S, Deshayes Kurt, Piotrowiak Piotr. Remote intermolecular "Heavy-atom effect": spin-orbit coupling across the wall of a hemicarcerand. J Am Chem Soc 2001;123:2444–5.
[49] Das P, Ghosh A, Das A. Unusual specificity of a receptor for Nd^{3+} among other lanthanide ions for selective colorimetric recognition. Inorg Chem 2010;49: 6909–16.
[50] Das P, Ghosh A, Bhatt H, Das A. A highly selective and dual responsive test paper sensor of Hg^{2+}/Cr^{3+} for naked eye detection in neutral water. RSC Adv 2012;2:3714–21.
[51] Chereddy NR, Suman K, Korrapati PS, Thennarasu S, Mandal AB. Design and synthesis of rhodamine based chemosensors for the detection of Fe^{3+} ions. Dyes Pigm 2012;95:606–13.
[52] Kim HN, Lee MH, Kim HJ, Kim JS, Yoon JY. A new trend in rhodamine-based chemosensors: application of spirolactam ring-opening to sensing ions. Chem Soc Rev 2008;37:1465–72.
[53] Mariana B, Carlos AMA, Jose MGM. Synthesis and applications of rhodamine derivatives as fluorescent probes. Chem Soc Rev 2009;38:2410–33.
[54] Ahamed BN, Ghosh P. An integrated system of pyrene and rhodamine-6G for selective colorimetric and fluorometric sensing of mercury (II). Inorg Chim Acta 2011;372:100–7.
[55] Suresh M, Mishra SK, Mishra S, Das A. The detection of Hg^{2+} by cyanobacteria in aqueous media. Chem Commun 2009:2496–8.
[56] Saha S, Chhatbar MU, Mahato P, Praveen L, Siddhanta AK, Das A. Rhodamine–alginate conjugate as self indicating gel beads for efficient detection and scavenging of Hg^{2+} and Cr^{3+} in aqueous media. Chem Commun 2012;48:1659–61.
[57] Saha S, Mahato P, Baidya M, Ghosh SK, Das A. An interrupted PET coupled TBET process for the design of a specific receptor for Hg^{2+} and its intracellular detection in MCF7 cells. Chem Commun 2012;48:9293–5.
[58] Nolan EM, Lippard SJ. Tools and tactics for the optical detection of mercuric ion. Chem Rev 2008;108:3443–80.
[59] Quang DT, Kim JS. Fluoro- and chromogenic chemodosimeters for heavy metal ion detection in solution and biospecimens. Chem Rev 2010;110:6280–301.
[60] Mahato P, Saha S, Suresh E, Liddo RD, Parnigotto PP, Conconi MT, et al. Ratiometric detection of Cr^{3+} and Hg^{2+} by a naphthalimide-rhodamine based fluorescent probe. Inorg Chem 2012;51:1769–77.
[61] Mahato P, Ghosh A, Saha S, Mishra S, Mishra SK, Das A. Recognition of Hg^{2+} using diametrically disubstituted cyclam unit. Inorg Chem 2010;49:11485–92.
[62] Saha S, Mahato P, Upendar RG, Suresh E, Chakrabarty A, Baidya M, et al. Recognition of Hg^{2+} and Cr^{3+} in physiological conditions by a rhodamine derivative and its application as a reagent for cell-imaging studies. Inorg Chem 2012;51:336–45.
[63] Suresh M, Mandal AK, Saha S, Suresh E, Mandoli A, Liddo RD, et al. Azine-based receptor for recognition of Hg^{2+} ion: crystallographic evidence and imaging application in live cells. Org Lett 2010;12:5406–9.
[64] Suresh M, Shrivastav A, Mishra S, Suresh E, Das A. A rhodamine-based chemosensor that works in the biological system. Org Lett 2008;10:3013–6.
[65] Suresh M, Mishra S, Mishra SK, Suresh E, Mandal AK, Shrivastav A, et al. Resonance energy transfer approach and a new ratiometric probe for Hg^{2+} in aqueous media and living organism. Org Lett 2009;11:2740–3.
[66] Mandal AK, Suresh M, Das P, Suresh E, Baidya M, Ghosh SK, et al. Recognition of Hg^{2+} ion through restricted imine isomerization: crystallographic evidence and imaging in live cells. Org Lett 2012;14:2980–3.
[67] Wang YH, Huang YQ, Li B. A cell compatible fluorescent chemosensor for Hg^{2+} based on a novel rhodamine derivative that works as a molecular keypad lock. RSC Adv 2011;1:1294–300.
[68] Zhao Y, Zheng BZ, Du J, Xiao D, Yang L. A fluorescent "turn-on" probe for the dual-channel detection of Hg(II) and Mg(II) and its application of imaging in living cells. Talanta 2011;85:2194–201.
[69] Bhalla V, Tejpal R, Kumar M. Rhodamine appended terphenyl: a reversible "off–on" fluorescent chemosensor for mercury ions. Sens Actuators B 2010; 151:180–5.
[70] Ma QJ, Zhang XB, Zhao XH. A highly selective fluorescent probe for Hg^{2+} based on a rhodamine-coumarinconjugate. Anal Chim Acta 2010;663:85–90.
[71] Ma TH, Zhang AJ, Dong M. A simply and highly selective "turn-on" type fluorescent chemosensor for Hg^{2+} based on chiral BINOL-Schiff's base ligand. J Lumin 2010;130:888–92.
[72] Yan FY, Cao DL, Yang N, Yu QH, Wang M, Chen L. A selective turn-on fluorescent chemosensor based on rhodamine for Hg^{2+} and its application in live cell imaging. Sens Actuators B 2012;162:313–20.
[73] Ghosh K, Sarkar T, Samadder A. A rhodamine appended tripodal receptor as a ratiometric probe for Hg^{2+} ions. Org Biomol Chem 2012;10:3236–43.
[74] Wang LN, Yan JX, Qin WW, Liu WS, Wang R. A new rhodamine-based single molecule multianalyte (Cu^{2+}, Hg^{2+}) sensor and its application in the biological system. Dyes Pigm 2012;92:1083–90.
[75] Hu ZQ, Yang XD, Cui CL. 1, 8-Anthrancene disulfonamide: a simple but highly sensitive and selective fluorescent chemosensor for Hg^{2+} in aqueous media. Sens Actuators B 2010;145:61–5.
[76] Zhao Y, Sun Y, Lv X, Liu YL, Chen ML, Guo W. Rhodamine-based chemosensor for Hg^{2+} in aqueous solution with a broad pH range and its application in live cell imaging. Org Biomol Chem 2010;8:4143–7.
[77] Wang HH, Xue L, Yu CL, Qian YY, Jiang H. Rhodamine-based fluorescent sensor for mercury in buffer solution and living cells. Dyes Pigm 2011;91:350–5.
[78] Wang HG, Li YP, Xu SF. Rhodamine-based highly sensitive colorimetric off-on fluorescent chemosensor for Hg^{2+} in aqueous solution and for live cell imaging. Org Biomol Chem 2011;9:2850–5.